

Transition radiation from particle showers

Juan Ammerman-Yebra,* Jaime Alvarez-Muniz and Enrique Zas

Instituto Galego de Física de Altas Enerxías (IGFAE)

Universidade de Santiago de Compostela, 15782 Santiago de Compostela, Spain

*E-mail: juan.ammerman.yebra@usc.es, jaime.alvarez@usc.es,
enrique.zas@usc.es*

When a particle shower goes through two different dielectric media, transition radiation is emitted. We present results obtained using the ZHS Monte Carlo across various scenarios, examining how the properties of the two media influence the resulting radio pulse. We also discuss the viability of the explanation of the ANITA anomalous events as transition radiation from a particle shower.

*10th International Workshop on Acoustic and Radio EeV Neutrino Detection Activities (ARENA2024)
11-14 June 2024
The Kavli Institute for Cosmological Physics, Chicago, IL, USA*

*Speaker

1. Introduction

The detection of ultra-high energy (UHE) neutrinos in the EeV energy range, is one of the big challenges in modern astrophysics. When UHE neutrinos interact in dense media the secondary particles from the interaction generate a particle shower that emits radio waves in the MHz-GHz band [1]. Current and planned experiments leverage the large effective volumes of ice on Earth, due to its high density and transparency to radio waves in the MHz-GHz regime [2], to detect these radio pulses emitted by the particle showers. Two primary approaches are employed for this detection: in-ice detection (as used by experiments like ARA [3], RNO-G [4] and IceCube Gen-2 radio [5]), and balloon-borne experiments (such as ANITA [6] and PUEO [7]) that observe the ice from high altitudes, measuring the refracted pulses.

These experiments can also observe the air-ice interface and are susceptible to events that produce radiation from showers developing in both media. Transition radiation is emitted when a particle crosses the boundary between two different dielectric media, generating a short pulse over a broad range of angles [8]. For high-energy showers, millions of charged particles cross the interface at various times and positions, resulting in a pulse that is highly dependent on the initial medium in which the shower develops.

In this study, we introduce a method for calculating transition radiation and investigate scenarios where particle showers transition from high-density (ice) to low-density media (air) and vice versa. Our analysis aims to understand the relationship between the properties of the two media and the resulting radio pulse.

2. Radio emission and transition radiation

Radio emission from a particle shower is calculated summing all the individual contributions to the electric field from charged particle tracks, the straight line segments each with constant velocity in which the particle trajectories are subdivided. The emission from one track is calculated with the ZHS algorithm [9], that gives the electric field in the frequency domain for an observer in the Fraunhofer limit or in the time domain version was developed [10], the latter requiring less computational power and most widely used. The ZHS algorithm in the time domain first calculates the vector potential and then, once the shower has fully developed, takes the minus time derivative to obtain the electric field. The expression for the vector potential of one track is:

$$\mathbf{A} = \frac{\mu e}{4\pi R} \mathbf{v}_\perp \frac{\Theta[t - \frac{nR}{c} - (1 - n\beta \cos \theta)t_1] - \Theta[t - \frac{nR}{c} - (1 - n\beta \cos \theta)t_2]}{(1 - n\beta \cos \theta)}, \quad (1)$$

where \mathbf{v}_\perp is the perpendicular velocity with respect to emission direction, n is the index of refraction, R is the distance from the track to the observer, c the speed of light, β the particle velocity divided by c , θ the angle between the emission direction and \mathbf{v} , and t_1 , t_2 the global times at the beginning and end of the track, respectively.

In order to calculate transition radiation we follow the approach in [11], sketched in Fig. 1. For the tracks fully contained in the medium where the observer is located, a direct and a reflected contribution are calculated. For the tracks fully contained in the other medium, a transmitted contribution is added, taking into account the refracted ray path. While the reflected contribution

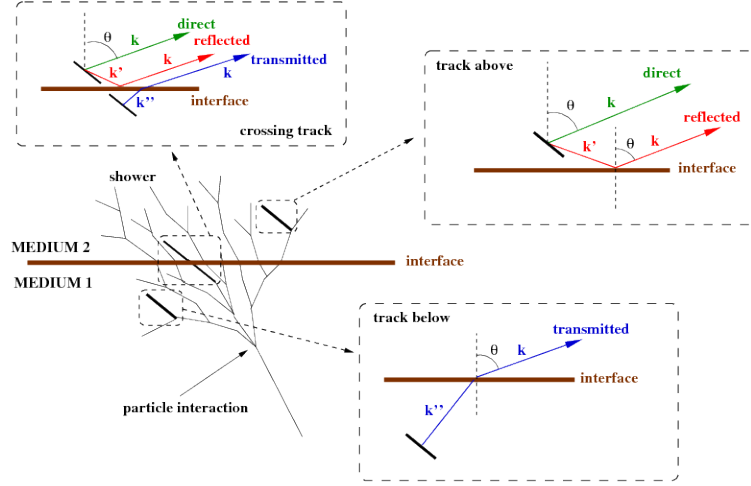


Figure 1: Sketch of the three contributions to the pulse from different particles tracks in a shower: a particle track contained in air (medium 1), a particle track contained in ice (medium 2) and a particle track crossing the interface. The latter is subdivided into two tracks each fully contained in a single medium. Taken from [11].

is obtained applying the standard Fresnel coefficients, for the transmitted contribution they are multiplied by a factor $n_2 \cos \theta / n_1 \cos \theta_{tr}$, where θ_{tr} is the transmitted angle, to into account that the rays emitted from a point source diverge when refracted [12]. For tracks that cross the boundary, the track is split at the interface and the calculation of the vector potential from the piece of track in the first medium is performed. Then, the particle properties are stored in a file for the vector potential calculation in the second medium. After that, we sum the final vector potentials of the two media and take the minus time derivative to obtain the total electric field. In this methodology, transition radiation arises from the fact that the contribution to the electric field from the two tracks before and after the interface, do not cancel out due to the different dielectric properties of the two media.

In this work we use the ZHS Monte Carlo [9] to obtain the radio emission from particle showers crossing developing in two media. The ZHS particle shower code simulates electromagnetic showers in dense homogeneous media. The interactions taken into account are: bremsstrahlung, pair production, Compton, Bhabba, Møller scattering and electron-positron annihilation. As particles propagate, the Monte Carlo also performs a continuous energy loss and multiple scattering calculation. The original ZHS Monte Carlo was later expanded to run in two adjacent media [11] and to allow for particle deflections in the presence of a magnetic field [13], two upgrades of the code that are crucial for a more realistic calculation of the radio emission crossing the atmosphere-ice interface and vice versa.

3. Transition radiation from ice to air

To study transition radiation emitted by a shower starting in ice and continuing development in air, we place observers in the air around the refracted Cherenkov cone emitted by the first part of the

shower in the ice. The coordinate system is such that the z -axis is perpendicular to the interface and the observers are placed in different positions along the x -axis at a height of 33 km as indicated in the left panel of Fig. 2. The magnetic field of the Earth is contained in the xz plane (with inclination 70° and magnitude 0.41 G). In this particular example, the shower is starting in ice and crossing into air around the depth of its maximum development X_{\max} . We choose the properties of the ice to be those of the vicinity of the surface, namely ice density 0.42 g cm^{-3} and index of refraction 1.36. For the properties of the atmosphere we took those at the altitude of Antarctica, with density $0.9095 \cdot 10^{-3} \text{ g cm}^{-3}$ and index of refraction 1.0002255.

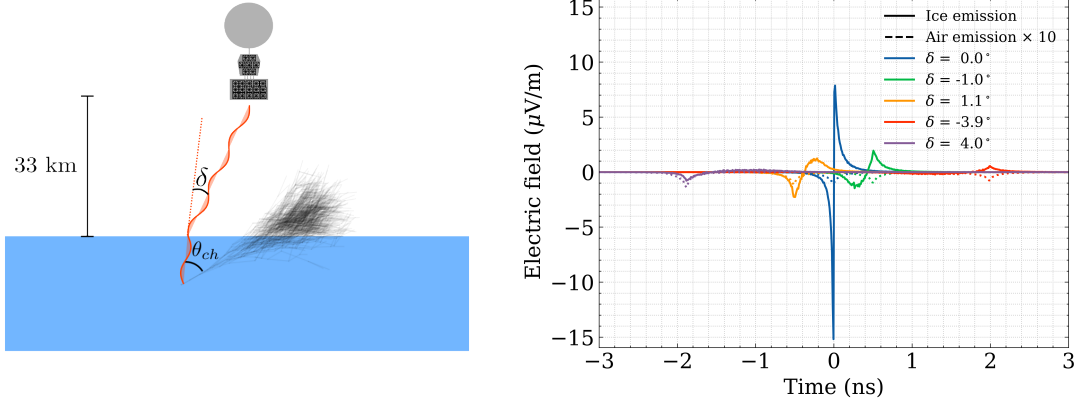


Figure 2: Left: sketch of the geometry used for the simulations of the shower developing from ice to air. Right: z -polarization of the electric field for the different observers placed at different angles θ_{obs} around the Cherenkov cone where $\delta = \theta_{ch} - \theta_{obs}$ with θ_{ch} the Cherenkov angle in ice, see left panel. The emission from the part of the shower developing in air has been multiplied by a factor 10 for easier readability.

In Fig. 2 we show the electric field for different observers for a 100 TeV electron-induced shower with zenith angle 60° . For the observer placed in the Cherenkov cone a sharp bipolar pulse, as expected from the Askaryan emission in ice, dominates the emission. Compared to the pulses from showers developing only in ice, this one has a higher frequency content, lasting only ~ 0.2 ns, due to the abrupt emission when the shower stops developing in ice. As the observer moves away from the Cherenkov cone the pulses are longer in time and lower in amplitude, as the observer no longer sees coherent emission from all the shower but mainly from the part of the shower that intersects the boundary between ice and air. There is also an inversion of the sharper part of the bipolar pulse due to transition radiation for observers inside and outside the Cherenkov cone. This is due to the time ordering that the observer sees depending on its angle relative to the Cherenkov cone. Observers inside the Cherenkov cone see the shower suddenly stopping its development in the ice first, followed by the emission coming from the ice. On the contrary, observers outside the cone see the emission of the shower in the ice first, and then that from the part abruptly finishing at the interface.

In Fig. 2 we have also plotted the contribution to the radiation of the part of the shower that develops in the air (dashed lines). In this particular example, the observers we have placed see the shower developing in air at angles $\sim 24^\circ$ with respect to the shower axis, that are far away from the expected coherent region of emission in air, at angles $\sim 1^\circ$ due to the low refractive index of air.

The contribution from air seen in Fig. 2 is dominated by transition radiation, as a pulse from an air shower could never be so short in time.

4. Transition radiation from air to ice

To compare the properties of transition radiation from a shower transitioning from air to ice to the previous case, we take an inclined (55° zenith) air shower and place observers in the x -axis around the reflected shower axis (left panel of Fig. 3) where the emission is expected to be coherent and more sizeable. In this geometry, the main contribution the observer sees is the reflected emission on the ice surface, since the direct and transmitted contributions are emitted at angles $\gg 1^\circ$ with respect to shower axis, where the emission is expected to be largely incoherent [14, 15]. Taking this into account, we do not include in the calculation the transmitted pulse from the part of the shower developing in the ice.

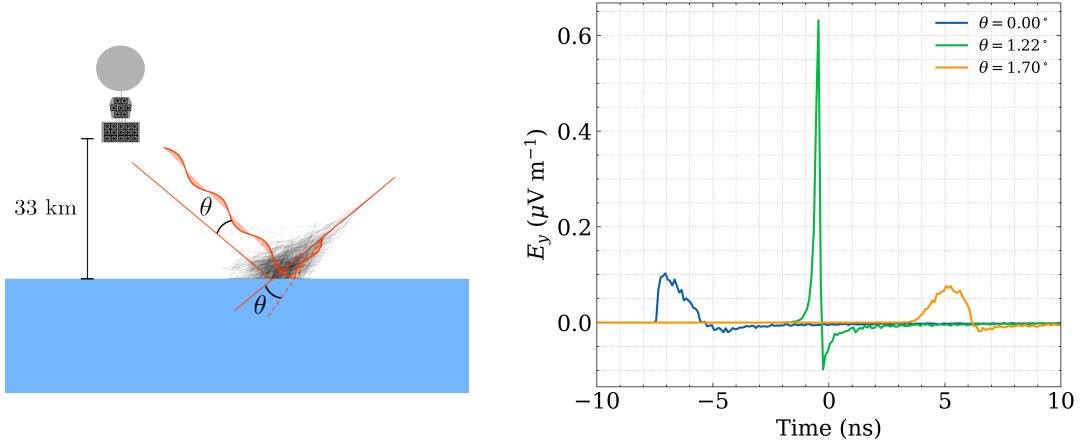


Figure 3: Left: Sketch of the geometry and observers used for the showers transitioning from air to ice. Right: y -polarization of the electric field emitted by a 1 PeV electron-initiated air shower that intersects the ice at X_{max} for an observer inside, outside and on the Cherenkov cone ($\theta = 1.22^\circ$).

The shower and media properties used in the following are consistent with those described in the previous section. The right panel Fig. 3 presents the pulses from a 1 PeV electron-initiated shower intersecting the ice at shower maximum, as observed by three different observers. Due to the density difference between air and ice that induce longer and wider showers in air, the resulting pulses are significantly longer in time compared to the previous scenario [13]. On the Cherenkov cone the pulse is high in amplitude and sharp in time, while for observers away from the cone the pulses are lower in amplitude and longer in time. For an observer inside the Cherenkov cone, the first peak exhibits a rapid rise followed by a gradual decline, while the reverse is true for the observer outside. To understand this behavior, we examine below the vector potential and the time delays of the shower front.

In Fig. 4 we show the time evolution of the vector potential for the pulses at the observer positions inside and outside the Cherenkov cone. The left panel (observer inside the Cherenkov cone) illustrates that, as the shower develops, contributions from later parts of the shower arrive

earlier, in particular the contribution from the abrupt end of shower development in air. However, we have checked that only the contribution from the most energetic particles is sizeable at early times. Less energetic particles accumulate larger time delays and contribute at later times. This causes the vector potential to exhibit a steep initial curve, resulting in a mostly monopolar pulse.

For the observer positioned outside the Cherenkov cone (right panel of Fig. 4), the contributions from the later parts of the shower arrive at later times as expected. On the other hand, the early stages of the shower barely contribute to earlier times in the vector potential. The reason for this behavior can be rooted to the time delays of the particles in the shower with respect to a particle traveling at the speed of light along shower axis. The delays at X_{\max} are typically of the order of ~ 10 ns, and as a result the time ordering of the contributions the observer sees are altered with respect to the ideal case of a particle traveling at the speed of light along the shower axis [13].

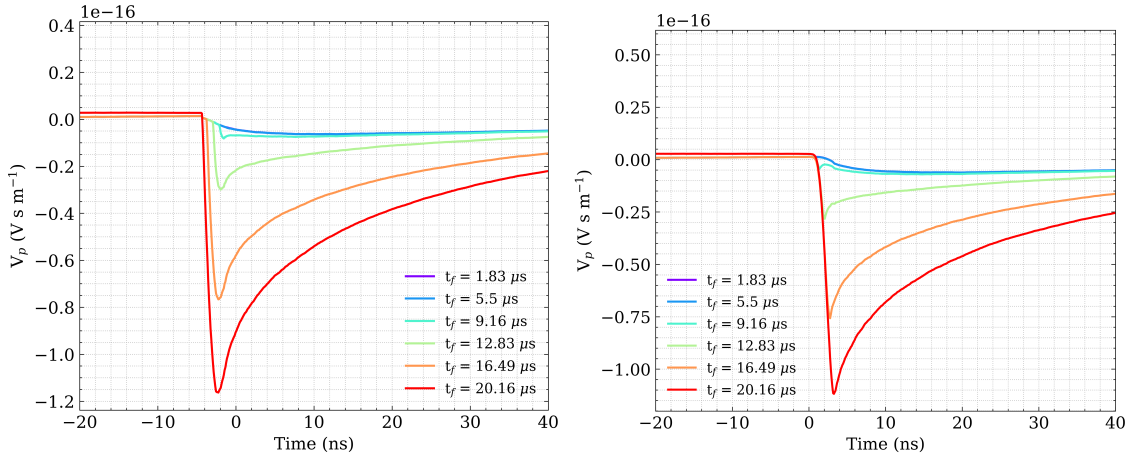


Figure 4: Left: Time evolution of the vector potential for an observer placed in the reflected shower axis (inside the Cherenkov cone) for an air shower starting in the air and transitioning into ice. Right: Same as left panel but for an observer at 1.7° away from the shower axis (outside Cherenkov cone). In all cases observers are placed at 33 km altitude.

Transition radiation from an air shower crossing into ice has been proposed as a possible explanation for the ANITA Anomalous Events (AAE) [14], that originate from directions typically associated with reflected cosmic rays, yet they do not exhibit the characteristic polarity inversion expected from such reflections. At the steep angles of the AEE ($\sim 30^\circ$ elevation), no particle within the Standard Model can travel through such amount of matter inside the Earth and produce an upward-going air shower that points to the detector [16, 17]. The authors of [14] suggest that when an air shower intersects the Antarctic ice sheet, the polarity of the observed pulses could vary depending on the observer's position relative to the shower axis. This idea is based on the time ordering of the sharp pulse due to transition radiation relative to the pulse from the rest of the shower. This part of the pulse is observed at earlier or later times when the observer is placed inside or outside the Cherenkov cone, as clearly shown in the right panel of Fig. 2 corresponding to the case of a shower transitioning from ice to air. However, there is no change in the polarity of the pulses, also for the case of a shower starting in air and developing in ice as shown in Fig. 3. In this case, there is again a reverse in the time ordering of the sharp pulse and that from the rest

of the shower as the observer crosses the Cherenkov cone. However the time ordering is not as clear as in the case of the shower developing from ice to air because the shower front delays cause contributions from different parts of the shower to mix, disrupting the expected time ordering of the shower development as perceived by the observer. The fact that the pulses do not change polarity, strongly disfavor the explanation for the AAE in [14]. Additionally, simulations accounting for the exponential atmospheric profile, instead of assuming an homogeneous atmosphere, also show no difference in the polarity of the pulses [15].

5. Conclusions

In this work, we have studied the radio emission from particle showers as they develop through different dielectric media. We have introduced the method used for calculating transition radiation with the ZHS algorithm. We have shown that the dielectric media properties affect significantly the shape of the radio pulse seen by observers inside and outside the Cherenkov cone. Despite this dependency on the properties, regardless of the medium's density, there is no polarity inversion for the different observers. The most notable effect occurs for a shower from ice to air, where depending on whether the observer is inside or outside the Cherenkov cone, the first or the second peak of the electric field gets enhanced with respect to the other one. The results obtained contribute to a better understanding of transition radiation from particle showers and its implications for the detection of ultra high energy cosmic rays and neutrinos from balloon-borne radio experiments. Considering our results, we strongly disfavor transition radiation as an explanation for the ANITA anomalous events.

References

- [1] G. A. Askar'yan, *Excess negative charge of an electron-photon shower and its coherent radio emission*, *Zh. Eksp. Teor. Fiz.* **41** (1961) 616.
- [2] S. Barwick, D. Besson, P. Gorham and D. Saltzberg, *South Polar in situ radio-frequency ice attenuation*, *Journal of Glaciology* **51** (2005) 231–238.
- [3] P. Allison, J. Auffenberg, R. Bard, J. Beatty, D. Besson, S. Böser et al., *Design and initial performance of the Askaryan Radio Array prototype EeV neutrino detector at the South Pole*, *Astroparticle physics* **35** (2012) 457.
- [4] J. A. Aguilar, P. Allison, J. Beatty, H. Bernhoff, D. Besson, N. Binglefors et al., *Design and sensitivity of the Radio Neutrino Observatory in Greenland (RNO-G)*, *Journal of Instrumentation* **16** (2021) P03025.
- [5] S. Hallmann, B. Clark, C. Glaser and D. Smith, *Sensitivity studies for the IceCube-Gen2 radio array*, *arXiv preprint arXiv:2107.08910* (2021) .
- [6] ANITA collaboration, *The Antarctic Impulsive Transient Antenna Ultra-high Energy Neutrino Detector Design, Performance, and Sensitivity for 2006-2007 Balloon Flight*, *Astropart. Phys.* **32** (2009) 10 [0812.1920].

- [7] Q. Abarr, P. Allison, J. A. Yebra, J. Alvarez-Muñiz, J. Beatty, D. Besson et al., *The payload for ultrahigh energy observations (PUEO): a white paper*, *Journal of Instrumentation* **16** (2021) P08035.
- [8] V. L. Ginzburg and I. M. Frank, *Radiation of a uniformly moving electron due to its transition from one medium into another*, *J. Phys. (USSR)* **9** (1945) 353.
- [9] E. Zas, F. Halzen and T. Stanev, *Electromagnetic pulses from high-energy showers: Implications for neutrino detection*, *Physical Review D* **45** (1992) 362.
- [10] J. Alvarez-Muñiz, A. Romero-Wolf and E. Zas, *Cherenkov radio pulses from electromagnetic showers in the time-domain*, *Phys. Rev. D* **81** (2010) 123009 [1002.3873].
- [11] P. Motloch, J. Alvarez-Muñiz, P. Privitera and E. Zas, *Transition radiation at radio frequencies from ultrahigh-energy neutrino-induced showers*, *Phys. Rev. D* **93** (2016) 043010 [1509.01584].
- [12] C. W. James, H. Falcke, T. Huege and M. Ludwig, *General description of electromagnetic radiation processes based on instantaneous charge acceleration in ‘endpoints’*, *Phys. Rev. E* **84** (2011) 056602 [1007.4146].
- [13] J. Ammerman-Yebra, J. Alvarez-Muñiz and E. Zas, *Density and magnetic field strength dependence of radio pulses induced by energetic air showers*, *JCAP* **08** (2023) 015 [2305.11668].
- [14] K. D. de Vries and S. Prohira, *Coherent transition radiation from the geomagnetically-induced current in cosmic-ray air showers: Implications for the anomalous events observed by ANITA*, *Phys. Rev. Lett.* **123** (2019) 091102 [1903.08750].
- [15] J. Ammerman-Yebra, J. Alvarez-Muñiz and E. Zas, *On the transition radiation interpretation of anomalous ANITA events*, *JCAP* **04** (2024) 030 [2311.05554].
- [16] ANITA collaboration, *Characteristics of Four Upward-pointing Cosmic-ray-like Events Observed with ANITA*, *Phys. Rev. Lett.* **117** (2016) 071101 [1603.05218].
- [17] ANITA collaboration, *Observation of an Unusual Upward-going Cosmic-ray-like Event in the Third Flight of ANITA*, *Phys. Rev. Lett.* **121** (2018) 161102 [1803.05088].